

Augmentor Combustion Instability with COMSOL Multphysics®

V. G. Shaw¹, J. D. Clabbers¹, E. J. Gutmark¹

1. Department of Aerospace Engineering & Engineering Mechanics, University of Cincinnati, Cincinnati, OH, USA

Introduction

Combustion instability occurs when oscillatory heat release rates couple with resonant chamber acoustics. The resulting positive feedback loop leads to intensified heat release and high amplitude pressure oscillations that can cause rapid component wear and engine failure in rocket and air breathing propulsion systems [1,2].

Self-excited combustion oscillations occur when energy is added to the acoustic field by heat release. According to the Rayleigh criterion [3], this occurs when the phase of heat release rate and acoustic pressure oscillations are within $\pm 90^\circ$. In real systems, damping must also be considered to determine if the oscillation is amplified.

Given the direct dependence of acoustic resonant modes on system geometry, real combustors can experience many different modes of combustion instability. In gas turbine afterburners, or augmentors, low frequency longitudinal oscillations propagate parallel to the flow direction and are commonly referred to as “rumble” or “buzz.” High frequency transverse oscillations, referred to as “screech,” propagate perpendicular to the flow direction.

When augmentor screech was first encountered in 1947, it was infrequent and considered to not be a serious issue [4]. However, by the 1950s, increased demands in augmentor performance required combustors to burn at higher fuel air ratios which brought about a greater tendency for screech [4,5]. By the end of the decade, it was found that increasing the damping potential of the augmentor through the use of a perforated liner was adequate for suppressing screech [5]. However, as modern augmentors increase in energy density and diameter, transverse modes become more prevalent while occurring at frequencies that fall below the effective range of perforated liners [6]. Therefore, a new method for preventing instability is needed.

Due to the high costs of operating full scale engines and the damaging nature of combustion instabilities, small scale test facilities that replicate the operating conditions of full scale engines provide a practical

means for studying combustion instability and instability suppression techniques.

Despite the relative geometric simplicity of small scale systems, the acoustic field accompanying combustion instability can be complex. While direct acoustic pressure measurements of combustors can be made, resolving mode shapes over a broad range of low and high frequencies requires dozens of pressure probes that can withstand the hostile combustor temperatures. These requirements greatly increase the complexities associated with detailed characterization of the acoustic field present during combustion instability.

COMSOL’s Pressure Acoustics, Frequency Domain, physics paired with an Eigenfrequency study is capable of solving the acoustic field in complex geometric and thermal environments. In this work, chamber acoustics are analyzed in a small scale augmentor simulation facility. Key results include the effect of a flame holder and temperature gradient on acoustic mode shapes and frequencies in an open-ended rectangular duct.

Experimental Set-up

The Combustion Wind Tunnel Facility (CWTF) at the University of Cincinnati generates conditions relevant to those encountered at the inlet of a jet engine augmentor. High speed air is preheated to a maximum temperature of 950 K using a J73 burner can supplied with Jet-A fuel. The CWTF features a 42.3” long test section with an 8” x 7” rectangular cross-section. Flow conditions entering the test section are measured in a 28.1” long inlet section. With the injection of unheated air into the plenum from a secondary air supply, inlet conditions reach Mach 0.3 (525 ft/sec at 965° F).

At certain operating conditions, flames stabilized with flame holders in the test section of the CWTF experience combustion instability at frequencies ranging from 100 Hz – 2300 Hz. While the oscillation mode of the flame can be inferred from frequency, operating conditions, high speed imaging, and an array of pressure transducers, measuring the entire acoustic field within the CWTF is a challenge.

COMSOL provides a means for rapidly computing the relevant acoustic field based on known experimental conditions.

Numerical Model

In a rectangular duct with open-ends, longitudinal standing waves form along the length of the duct with acoustic pressure nodes (velocity antinodes) at each open-end. The longitudinal mode number corresponds to the number of acoustic pressure antinodes (velocity nodes) inside the duct. Transverse standing waves form across the duct with pressure antinodes at the walls with the mode number being the number of pressure nodes between the walls. The frequency of the sinusoidal pressure distribution for both longitudinal and transverse waves corresponds to the mode frequency. For rectangular ducts with closed-ends, the frequency of a standing waves ($f_{l,m,n}$) is readily calculated using Eq. 1 [7] where c is the speed of sound, and l , m , and n are the mode numbers in the length (L), width (W), and height (H) dimensions, respectively.

$$f_{l,m,n} = \frac{c}{2} \sqrt{\left(\frac{l}{L}\right)^2 + \left(\frac{m}{H}\right)^2 + \left(\frac{n}{W}\right)^2} \quad (1)$$

However, Eq. 1 fails predict mode frequencies as it is applied to more complex geometric and fluid dynamic environments such as those encountered in the CWTF.

The model domain without the flame holder is reduced to a rectangular duct with dimensions corresponding to the combined inlet and test section of the experimental facility ($L = 64.1'' \times H = 8'' \times W = 7''$). The working fluid in this study was air as defined by the built-in materials in COMSOL.

When a flame is stabilized in the test section of the CWTF, a severe temperature gradient exists. This was implemented in the computational model by defining a separate “flame domain” which linearly expands from the downstream face of the flame holder to a width of 3.5” at $y = 64.1''$. The expansion of the flame domain was done to approximate flame spread downstream of the flame holder. Alterations to the simple duct domain that include the flame holder and flame domain are shown in Figure 1.

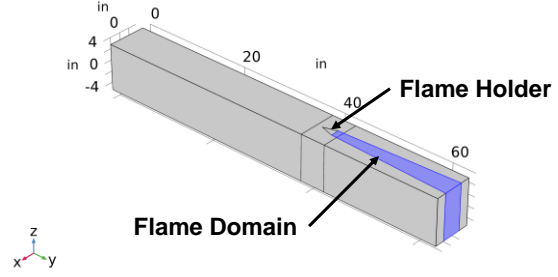


Figure 1. Model geometry with flame holder and flame domain (highlighted).

The Pressure Acoustics, Frequency Domain physics interface was used to solve the Helmholtz equation (Eq. 2) in the frequency domain. The Eigenfrequency study was then used to compute the eigenfrequencies and eigenmodes of the model. The eigenfrequencies correspond to the resonant frequencies of the system while the respective eigenmode represents the normalized acoustic field for that frequency.

$$\nabla \cdot \left(-\frac{1}{\rho} (\nabla p_t - \mathbf{q}_d) \right) - \frac{k_{eq}^2 p_t}{\rho} = Q_m \quad (2)$$

$$p_t = p + p_b, k_{eq}^2 = \left(\frac{\omega}{c}\right)^2, -i\omega = \lambda$$

Open-end, or “Sound Soft,” boundary conditions ($p_t = 0$) were assumed for both the inlet and outlet faces of the domain due to area expansions located just upstream and downstream of the CWTF inlet and test section, respectively. Closed-end, or “Sound Hard (Wall),” boundary conditions (Eq. 3) were used for the walls along the length of the duct and the walls of the flame holder. An initial value for pressure of $p = 0 \text{ Pa}$ was used throughout this study in all domains.

$$-\mathbf{n} \cdot \left(-\frac{1}{\rho} (\nabla p_t - \mathbf{q}_d) \right) = 0 \quad (3)$$

A flame holder was included by subtracting the flame holder cross-section through the 8” dimension of the computational domain. The flame holder was an isosceles triangle with a base width of 1.5” and a streamwise length of 2.38”. The upstream tip of the triangular flame holder was located at $x = 0''$, $y = 40''$.

The grid for the empty rectangular duct was a user defined free tetrahedral mesh based on the “Extremely Fine” mesh option. Reducing the maximum element size to 0.75” resulted in a mesh of 197,164 elements. Decreasing the maximum element size to 0.5” and 0.4” resulted in 485,044 and 956,608

elements, respectively. No change in mode shape was observed as element size was decreased while variance in frequency was a maximum of 0.01 Hz between the smallest and largest element sizes. Therefore, it was determined that the element size of 0.75" was sufficient for resolving the acoustic field of the duct.

Additional mesh refinement was added for the cases with the flame holder and temperature gradient (Figure 2). Reduced element size was applied to the volume 1" upstream and downstream of the flame holder to account for the geometric discontinuity of the flame holder. Refinement was also added to the flame domain to ensure solution accuracy across the temperature gradient of the flame domain.

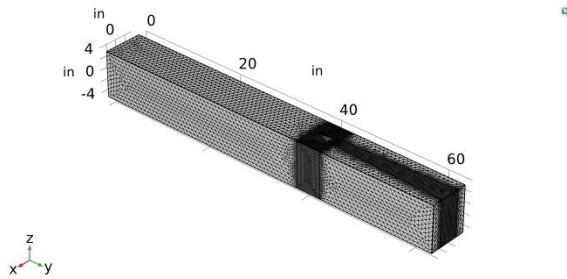


Figure 2. Mesh refinement added for the flame holder and temperature gradient regions.

While no changes in mode shape were observed as refinement was added to these regions, decreasing from the baseline maximum element size of 0.75" to 0.25" and 0.30" around the flame holder and inside the flame domain resulted in changes in frequency less than 0.01 Hz. The meshed domain consisted of 716,599 tetrahedral elements.

Simulation Results

Open-end Rectangular Duct, No Flame Holder

The calculated pressure distribution for the first 4 longitudinal modes along the cross-sectional centerline ($x = 0, z = 0$) at a temperature of 293.15 K are shown in Figure 3a. As described by acoustic theory, acoustic pressure nodes exist at both open-end boundaries ($y = 0$ " and $y = 64.1$ "") for each longitudinal mode and the mode number equals the number of pressure antinodes along the duct. The first longitudinal mode is a half-wave with a single pressure antinode halfway along the length of the duct ($y = 32.05$ "") with an eigenfrequency of 105.4 Hz. For any higher order longitudinal mode, the eigenfrequency can be approximated by multiplying the first order eigenfrequency by the respective mode number. Eq. 1 produced the same eigenfrequency for

the first 4 longitudinal modes despite being defined for closed-end ducts. Therefore, when applying Eq. 1 to an open-end duct, the correct boundary conditions must be considered to determine the correct mode shape.

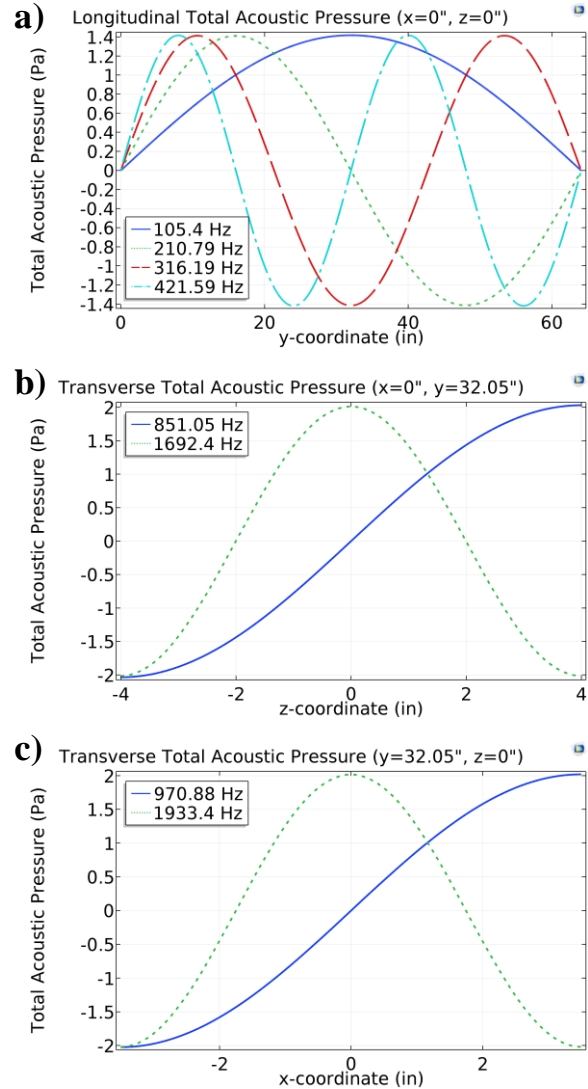


Figure 3. Acoustic pressure distribution in the empty duct at 293.15K for the a) first 4 longitudinal modes and the first 2 transverse modes in the b) 8" and c) 7" dimensions.

The lateral distribution of acoustic pressure for the first 2 transverse modes across the 8" and 7" dimensions are shown in Figure 3b-c. Transverse modes have pressure antinodes at the walls with the number of pressure nodes between the walls corresponding to the transverse mode number. The shorter length of the duct in both transverse dimensions results in transverse modes with frequencies much higher than the first several longitudinal modes. Given that the duct is 1" taller

than it is wide, any transverse mode in the 8" dimension will have a lower frequency than the corresponding mode in the 7" dimension. Eq. 1 was found to under predict transverse mode eigenfrequencies for the open-end duct. This is due to the addition of a first order longitudinal component to the transverse mode caused by the open-end inlet and outlet boundary conditions. This is shown for the first transverse modes in each dimension in Figure 4a-b as the streamwise distribution of acoustic pressure varies as a half-wave. It should be noted that when run with closed-end boundary conditions, COMSOL transverse eigenfrequencies are equal to those calculated from Eq. 1.

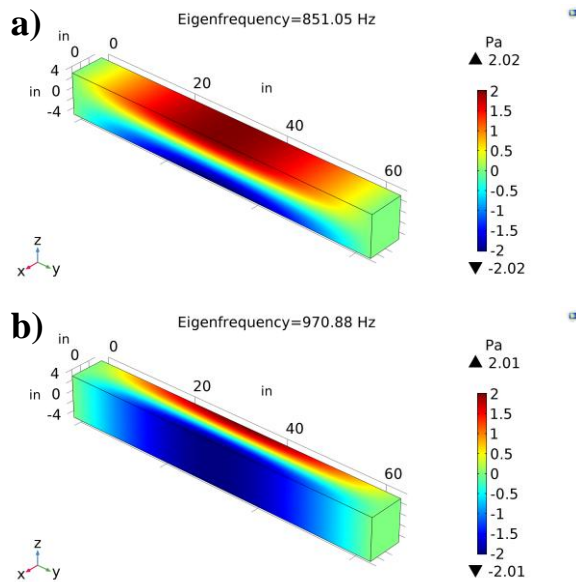


Figure 4. Acoustic pressure for the first transverse modes in the a) 8" and b) 7" dimensions without the flame holder.

Increasing the temperature within the duct resulted in increased eigenfrequencies while mode shapes were unchanged. Increased temperature increases sound speed which increases mode frequency as described in Eq. 1.

The Addition of a Flame Holder

With the ability of COMSOL to properly calculate the acoustic field confirmed, the impact of including a flame holder in the domain is now considered. Although the flame domain was included in the geometry, both the flame domain and the upstream domain were kept at 293.15 K to isolate the changes caused by the addition of the flame holder.

For longitudinal modes, the addition of a triangular flame holder to the domain does not significantly alter resonant frequencies and mode shapes. This is

shown in Figure 5 where only a slight change in eigenfrequency is observed for each of the first 4 longitudinal modes. The only apparent change along the centerline mode shape is a discontinuity that occurs at the flame holder between $x = 40"$ and $x = 42.38"$. However, the pressure field quickly recovers its upstream behavior downstream of the flame holder. This shows that the flame holder, despite imposing a cross-sectional blockage of 21.4%, is effectively transparent to longitudinal modes. Longitudinal acoustic energy passes around the flame holder with the only observed change being a minimal change in resonant frequency.

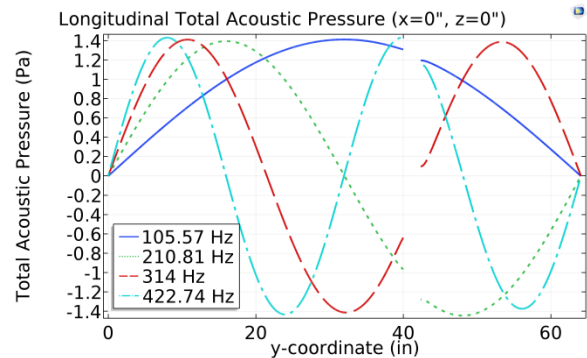


Figure 5. Acoustic pressure distribution in the duct with a flame holder at 293.15K for the first 4 longitudinal modes.

However, it does appear that the position of the flame holder with respect to mode shape does impact the observed shift in resonant frequency when compared to the empty duct. For the first, second, and fourth longitudinal modes, the flame holder position is near an acoustic pressure antinode and results in a slight increase in resonant frequency. For the third longitudinal mode, the flame holder is positioned near an acoustic pressure node and results in a decrease in resonant frequency. This behavior was also observed for higher order longitudinal modes.

Given that the flame holder consists of solid walls, boundary conditions require acoustic pressure antinodes normal to its surfaces. Therefore, when a longitudinal standing wave forms in the duct with the flame holder present, the acoustic field changes to best satisfy the boundary condition at both the flame holder and the inlet and outlet "sound soft" boundaries. If a longitudinal mode has an antinode near the flame holder, the wavelength will decrease to maintain elevated acoustic pressure across the flame holder. Alternatively, if a longitudinal mode occurs such that a node forms near the flame holder, the wavelength decreases to shift regions of higher acoustic pressure closer to the flame holder.

Similar to longitudinal modes, transverse standing waves in the 8" dimension showed minimal changes in mode frequency and shape with the addition of the flame holder to the domain (Figure 6). While the small shift in frequency can be attributed to the longitudinal component of the mode, the transverse component of the mode is parallel to the walls of the flame holder and is unaffected by the flame holder wall boundary conditions.

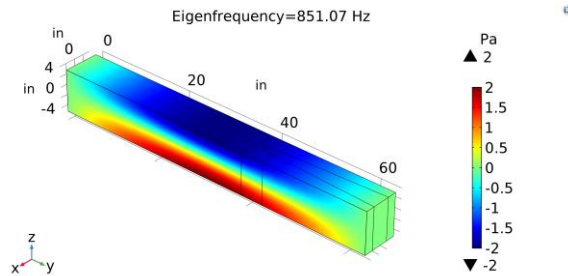


Figure 6. Acoustic pressure field for the first transverse mode in the 8" dimension with the flame holder.

However, transverse standing waves across the 7" dimension showed substantial changes in both mode frequency and shape with the addition of the flame holder. Without the flame holder in the duct, the first transverse mode in the 7" dimension existed throughout the longitudinal dimension of the duct as shown in Figure 4b. However, with the addition of the flame holder, the first transverse mode in the 7" direction concentrates locally around the flame holder (Figure 7). Both upstream and downstream of the flame holder, the longitudinal component of the transverse mode tapers towards the domain walls at approximately the flame holder half-angle. High pressure regions that are 180° out-of-phase with each other extend from the upstream angled walls of the flame holder to the walls of the domain. The existence of 180° out-of-phase elevated pressure on the surfaces of the flame holder provides potential insight into combustion instability coupling mechanisms between duct acoustics and fluid dynamics in the current geometry.

Previous small scale experimental studies have shown that transverse screech instabilities are driven by 180° out-of-phase vortex shedding across the width dimension of the flame holder [5,7,8]. Given that the origin of vortex shedding is due to the formation of a boundary layer on the flame holder surfaces [9], the formation of 180° out-of-phase pressure regions on the flame holder surface could perturb the boundary layer such that vortices are shed in an alternating fashion. This would result in the periodic transport of fresh reactants into the wake of the flame holder which leads to oscillating heat

release as described in [8]. If the ignition time delay of the vortex is such that heat release is in phase with the acoustic field, the instability will be amplified.

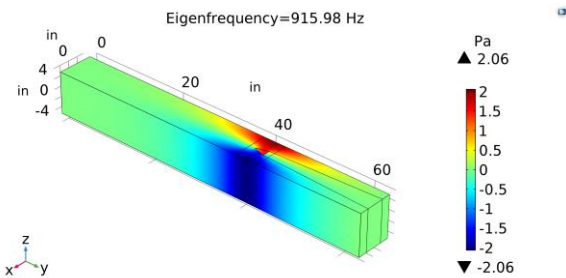


Figure 7. Acoustic pressure field for the first transverse mode in the 7" dimension with the flame holder.

The unique shape of the acoustic field both upstream and downstream of the flame holder also provides interesting implications for transverse combustion instability. The upstream portion of the mode could periodically force transverse fuel and velocity distributions to help drive the instability. Downstream of the flame holder, the shape of the transverse mode is similar to the typical V-shaped flame stabilized by a bluff body. This could allow the acoustic field to interact directly with the flame surface. The drop in acoustic pressure amplitude downstream of the flame holder reinforces the notion that the driving mechanisms of the instability occur close to the flame holder [8].

Temperature Gradient Effects

When a flame is established downstream of the flame holder, a large temperature gradient exists. Given the dependence of sound speed on temperature, Eq. 1 shows that mode frequencies will increase with temperature. However, Eq. 1 can only account for thermal gradients by assuming an effective global temperature based on both the upstream temperature and the amount of fuel available for combustion downstream of the flame holder. This approach typically requires several iterations and assumptions that are guided by experimental data that still fails to accurately determine mode shapes.

Adding a region of elevated temperature downstream of the flame holder provides a simplified means for simulating a flame stabilized by the flame holder. In the current study, the flame domain expanded linearly from the lips to an outlet width of 3.5" and was set to 1600 K. The upstream temperature was kept at 293.15 K.

For longitudinal modes, the primary impact of the temperature gradient is to slightly increase mode frequencies due to an increase in sound speed within the flame domain. Upstream of the flame holder the longitudinal mode is primarily influenced by the upstream temperature. However, downstream of the flame holder, the amplitude of longitudinal modes decreases (Figure 8). The upstream conditions appear to have a dominating effect on the mode frequency as the calculated eigenfrequencies approach that of the upstream temperature. This is expected due to the larger volume of lower temperature domain. In systems where the flame zone covers the majority of the domain, such as a real gas turbine augmentor, the effective temperature will approach that of the flame.

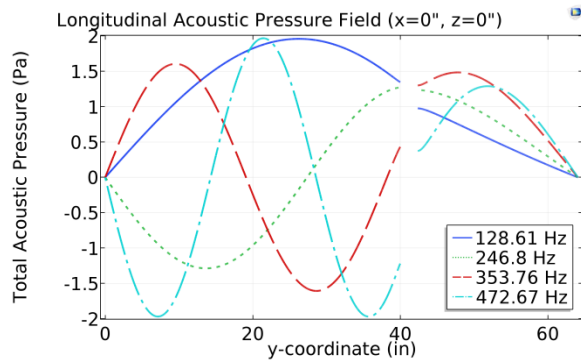


Figure 8. Acoustic pressure distribution in the duct with the flame holder and temperature gradient for the first 4 longitudinal modes.

As with longitudinal modes, transverse mode eigenfrequencies were also observed to increase due to increased sound speed within the flame domain. However, the most prominent impact of the temperature gradient on the transverse acoustic field was to concentrate the longitudinal component of the first order modes upstream of the flame holder. This is shown in the 8th dimension in Figure 9.

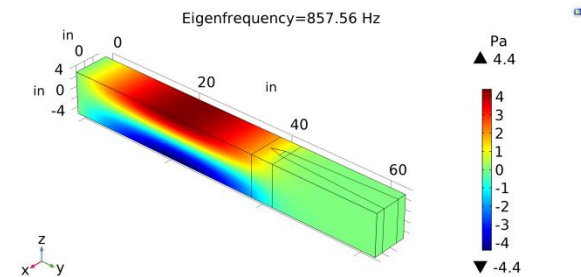


Figure 9. Acoustic pressure field for the first transverse mode in the 8th dimension with the flame holder and temperature gradient.

While the longitudinal component of the first transverse mode in the 7th dimension was also concentrated upstream of the flame holder, the overall mode shape changed considerably with the addition of the temperature gradient. Without the temperature gradient, the first mode in the 7th direction concentrated around the flame holder with equal upstream and downstream spread. While 180° out-of-phase regions of increased pressure remain on the surfaces of the flame holder, the addition of the temperature gradient shrinks and extends the downstream and upstream extents of the mode, respectively (Figure 10). In this instance the temperature gradient appears to break the longitudinal symmetry of the mode and shifts downstream acoustic energy upstream away from the flame domain.

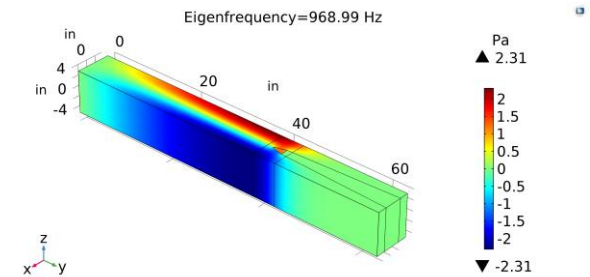


Figure 10. Acoustic pressure field for the first transverse mode in the 7th dimension with the flame holder and temperature gradient.

The capability of the first transverse mode in the 7th direction to interact with the flame appears to be greatly reduced. With the downstream extent of the mode reduced by the temperature gradient, oscillatory heat release must occur much closer to the flame holder to effectively add energy to the acoustic field. However, due to the elevated temperatures of the flame, ignition time delay is reduced [8]. This reduces the transport distance of reactants prior to ignition, thereby maintaining the potential for oscillatory heat release near the flame holder and the high amplitude regions of acoustic pressure.

While the current results provide interesting insights into duct acoustics and flames stabilized by bluff bodies, the inability of the current method to show changes in the acoustic field as it couples with the flame limits the application of these results to steady conditions preceding the transition to coupled combustion instability.

Mode Transition

In addition to simple modes like those described throughout this work, many combined modes exist in

the system where standing waves form in multiple dimensions of the duct simultaneously. There are a few instances in which combined modes induce interesting behavior in the system with the flame holder and temperature gradient. An example of this is shown in Figure 11 where a combined longitudinal and transverse mode transitions to an effective transverse mode downstream of the flame holder. This behavior has been reported in experimental and computational results in [10].

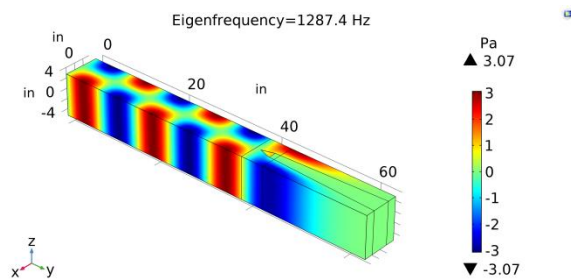


Figure 11. Mode transition downstream of the flame holder with temperature gradient.

With the goal of developing instability suppression strategies in mind, one cannot be certain that a strategy that suppresses a combined mode will work for a pure transverse mode. Therefore, combustion instability characterization efforts should consider the acoustic field both upstream and downstream of the flame holder when determining the mode of oscillation.

Conclusions

The effects of integrating a flame holder and temperature gradient on the acoustic field in a small scale augmentor test facility were simulated with COMSOL Multiphysics® software. Transverse modes were observed to have a longitudinal component with frequencies higher than those calculated with Eq. 1. When a flame holder was added to the domain, minimal changes in longitudinal mode shape and frequency were observed. This was also the case for the first transverse mode in the 8" dimension. However, the first transverse mode in the 7" dimension changed significantly with the addition of a flame holder. The acoustic field concentrates around the flame holder with regions of 180° out-of-phase elevated pressure amplitude on the surfaces of the flame holder. This feature of the acoustic field can help describe asymmetric vortex shedding observed during screeching combustion.

The addition of a temperature gradient downstream of the flame holder shifts the acoustic field upstream while slightly increasing mode frequencies. Instances

of mode transition suggest the need for detailed characterization of the acoustic field both upstream and downstream of the flame holder to properly determine the mode of combustion oscillations.

Ongoing efforts to implement flow and heat transfer effects should aid in further replicating instability conditions observed in the experimental facility. Future parametric studies will continue to analyze the impact of flame holder geometry and temperature gradients on mode frequency and shape. COMSOL's Application Builder is being used to develop a user friendly interface for analyzing acoustics in various combustion chamber geometries including full scale gas turbine augmentors.

References

- 1 Crocco, L., and Cheng, S. I., "High frequency combustion instability in rockets with distributed combustion," *Symposium (International) on Combustion*, vol. 4, 1953, pp. 865–880.
- 2 Lundin, B. T., Gabriel, D. S., and Fleming, W. A., *Effect of Operating Conditions and Design on Afterburner Performance*, Langley Field: 1956.
- 3 Strutt, John William, B. R., *The Theory of Sound*, Macmillan, 1896.
- 4 Usow, K. H., Meyer, C. L., and Schulze, F. W., "Experimental Investigation of Screeching Combustion in Full-Scale Afterburner," *NACA Research Memorandum*, vol. RM E53101, 1953.
- 5 Lewis Laboratory Staff, *A Summary of Preliminary Investigations into the Characteristics of Combustion Screech in Ducted Burners*, 1958.
- 6 Lovett, J. A., Brogan, T. P., Philippona, D. S., Keil, B. V., and Thompson, T. V., "Development Needs for Advanced Afterburner Designs," *40th Joint Propulsion Conference*, vol. 40, 2004, pp. 1–12.
- 7 Blackshear, P. L., Rayle, W. D., and Tower, L. K., "Experimental Determination of Gas motion Accompanying Screeching Combustion in a 6-Inch Simulated Afterburner," *NACA Research Memorandum*, 1953.
- 8 Rogers, D. E., and Marble, F. E., "A mechanism for high frequency oscillations in ramjet combustors and afterburners," *Jet Propulsion*, vol. 26, 1956, pp. 456–462.
- 9 Bearman, P. W., "Vortex Shedding from Oscillating Bluff Bodies," *Ann. Rev. Fluid Mech.*, vol. 16, 1984, pp. 195–222.
- 10 Ghani, A., Poinso, T., Gicquel, L., and Staffelbach, G., "LES of longitudinal and transverse self-excited combustion instabilities in a bluff-body stabilized turbulent premixed flame," *Combustion and Flame*, vol. 162, 2015, pp. 4075–4083.